

DIGITAL ACCESS TO SCHOLARSHIP AT HARVARD
DASH.HARVARD.EDU



HARVARD LIBRARY
Office for Scholarly Communication

Dissecting FRGY: Characterization of Specific FRGY2A/B Isoforms in Relation to Protein-Protein Interactions and Translational Masking.

The Harvard community has made this article openly available. Please share how this access benefits you. Your story matters

Citation	Cumming, Andrew. 2019. Dissecting FRGY: Characterization of Specific FRGY2A/B Isoforms in Relation to Protein-Protein Interactions and Translational Masking.. Master's thesis, Harvard Extension School.
Citable link	http://nrs.harvard.edu/urn-3:HUL.InstRepos:42006713
Terms of Use	This article was downloaded from Harvard University's DASH repository, and is made available under the terms and conditions applicable to Other Posted Material, as set forth at http://nrs.harvard.edu/urn-3:HUL.InstRepos:dash.current.terms-of-use#LAA

Dissecting FRGY: Characterization of Specific FRGY2A/B Isoforms In Relation to Protein-Protein Interactions and Translational Masking.

Andrew Cumming

A Thesis in the Field of Biotechnology

for the Degree of Master of Liberal Arts in Extension Studies

November 2019

Abstract

The aim of this project is to investigate the binding properties and functions of three isoforms of the mRNA-binding protein FRGY2: FRGY2A1, FRGY2A2, and FRGY2B (referred to collectively here as FRGY2A/B). Previous research has mainly addressed FRGY2A/B as one large group, but there may be important differences between the known isoforms. Constructs were designed to express His-tagged FRGY2A/B isoforms in E. coli for Ni^{2+} column purification by FPLC, and constructs designed for expression in *in vitro* transcription and translation systems. Spectrophotometric data from the purification process, and additional crosslinking provides compelling evidence that FRGY2A/B isoforms self-interact and form multimeric complexes through weak interactions. Further co-immunoprecipitation suggests that isoforms, particularly FRGY2A1 and FRGY2A2 interact with one another, irrespective of phosphatase or kinase treatment. Functional experiments show transcriptional masking in *in vitro* transcription and translation assays. In this setting, masking appears enhanced by dephosphorylation by calf intestinal phosphatase.

Dedication

To my wife Mary, whose support made this project possible. To my daughter River, whose curiosity is a constant inspiration. To my son Stellan, who arrived in our family mere weeks ago and is a constant reminder of our potential for growth.

Acknowledgments

I offer my deepest thanks to Dr. Alain Viel, for his guidance and help throughout this project. Thanks are also due to undergraduate students Edward Lee, who worked alongside me for a substantial part of this project, and Christine Zheng, Abby Joseph, and Hagen Puller for providing preliminary research.

Table of Contents

Abstract ……...iii

Dedication ……...iv

Acknowledgments …….. v

List of Tables …….. viii

List of Figures ……ix

I. Introduction …… 1

Function …….. 1

mRNA Binding ……... 5

Translational Masking ……..... 6

Nucleolar Dynamics ……8

FRGY2A/B and Disease ……9

II. Materials and Methods ……..... 12

III. Results ……...19

Interaction of FRGY2A/B ……...19

FPLC ……... 19

Nucleic Acid Binding ……. 21

Antibody Characterization ……..22

Co-Immunoprecipitation ……... 23

Phosphorylation/Dephosphorylation …….. 24

IV. Discussion ……... 27

Protein-Protein Interactions ……..... 27

RTS Inhibition …… 31

Conclusions …… 33

Future Research …….. 34

References …….. 37

Appendix I …….. 40

Appendix II …… 43

List of Tables

Table 1: Primer sequences for construction of FRGY2A/B plasmids.

Table 2: Steps for Ni^{2+}-column FPLC purification of His-tagged FRGY2A/B.

Table 3: Antibody information.

Table 4: Mass Spectrometry Analysis of FRGY2A2 Treated with Phosphatase (CIP) and Kinase (CK2)

List of Figures

Figure 1: System Traces of FRGY2A/B Purification by FPLC

Figure 2: SDS-PAGE of FPLC Fractions Containing Eluted FRGY2A1-CT-His

Figure 3: DMP crosslinking of purified FRGY2A1

Figure 4: Re-injection and FPLC fractionation of previously-purified FRGY2B

Figure 5: Assessment of stability of FRGY2A2 self-complexing

Figure 6: Second-stage FPLC re-run of FRGY2B Peak 2 and Peak 5

Figure 7: RNase and DNase Treatment of FPLC-purified FRGY2A1

Figure 8: Test of FRGY2A/B antibody sensitivity and specificity

Figure 9: Co-immunoprecipitation with FRGY2A1

Figure 10: Co-immunoprecipitation with FRGY2A2

Figure 11: *In vitro* Phosphorylation and Dephosphorylation of FRGY2A1 and FRGY2A2

Figure 12: Mass Spectrometry Analysis of FRGY2A1 Treated With Kinase and Phosphatase

Figure 13: Translation Inhibition via Phosphate-Modified FRGY2A1 and FRGY2A2

Figure S1: Schematic diagram depicting the structure of the Y-box protein

Figure S2: Alignment between FRGY1, FRGY2b, FRGY2A1 and FRGY2A2

Figure S3: Schematic map of FRGY2A/B constructs in pET303-CT-His

Figure S4: Flow cytometry analysis of nuclei

Figure S5: FRGY2A1 Nuclear Transport

Chapter I

Introduction

FRGY (pronounced “froggy”) was initially discovered through its ability to mask mRNA and block gene expression at the translational level. Throughout the literature, FRGY2 is often treated as a single protein, though it appears that there are at least three different isoforms. Of interest here are FRGY2A-1, FRGY2A-2, and FRGY2B (collectively referred to as FRGY2A/B). They share a common trait – they are members of the Y-Box Binding family (like all members of the FRGY family), and are able to bind to mRNA and inhibit translation (Sommerville & Ladomery, 1996).

In terms of the sequence of FRGYA/B, alignment of FRGY2A1, FRGY2A2, and FRGY2B show shared sequence between FRGY2A1 and FRGY2A2 at the C-terminus, with some divergence from FRGY2B as well (Figure S1). This is significant because prior studies have examined FRGY2 as a group. Since the differences between FRGY2 variants are within the centers of RNA binding, it is possible that small differences in protein sequence could have significant impact on RNA binding ability and specificity. In addition, these differences may also affect protein-protein interactions. Since FRGY2A/B appears to have multiple roles and is a part of the mRNP complex, differences in interactions may provide insight to its specific functions.

In addition to cellular function and binding specificity, different FRGY2A/B isoforms may also exhibit variation in dosage response. One factor separating the role of FRGY2A/B as a transcription factor from that of a translational repressor is dosage – in low amounts, it acts as the former, and in larger amounts, the latter. Again, to this point, FRGY2A/B has largely been studied as a single group. Separating out the different isoforms may reveal hidden complexity in what, as a whole, appears to be a simple dose response. For example, is the dosage of a specific isoform responsible for a given response? Or are the ratios between FRGY2A/B important to activity?

The presence of homologous genes between species and paralogous genes within species - each with distinct behaviors and roles – adds plausibility to any functional distinction between FRGY2A/B isoforms. Explored later in this proposal in greater detail, these related Y-box binding proteins also have clinical relevance, as they are play specific roles in cell proliferation and cancer, as well as reproduction and fertility. While particular clinical aspects of FRGY2A/B are outside of the scope of this project, the distinct behaviors of highly-similar mRNP components make more targeted investigation into FRGY2A/B worthwhile. More subtle functions may be averaged out or masked when examined in the aggregate, but brought out upon addition of targeted and specific application of FRGY2A/B isotypes and fragments.

My overall goal in this project is to examine the properties of FRGY2A-1, FRGY2A-2, and FRGY2B separately. In doing so, I hope to shine a light on the functions of FRGY2 variants and determine whether the commonly accepted

functions of FRGY2A/B can be attributed to specific components, variants, or combinations thereof.

My hypothesis is that many of the attributes of FRGY2A/B as a whole, can be assigned to specific isoforms, and even to isoform-specific domains. Specifically, I predict that there will be variation between RNA binding ability and specificity between the CSDs, and that the variant N-terminal domains will exhibit variability in translation inhibition and possibly protein-protein interactions.

Function

One of the primary functions of FRGY2A/B appears to be the regulation of maternal mRNAs, protecting and storing them for later use during early oogenesis. During this stage, the developing embryo has not yet begun new transcription, and relies on pre-existing maternal mRNA transcribed during oogenesis, and thus transcriptional control over gene expression is nonexistent (Mostafa, et al., 2009). Furthermore FRGYA/B affects the nucleolus and progression of the cell cycle.

In keeping with its function, FRGY2A/B is a member of the messenger ribonucleoprotein (mRNP) complex. The mRNP complex is what its name suggests – a protein complex that binds to mRNA. First discovered in the mid-1950s, the mRNP complex was further examined and characterized over the following decades (Dreyfuss, 1986). As a broad category of complexes, rather

than a single entity, mRNP complexes involve over a thousand different interacting components affecting mRNP activity (Singh, Pratt, Yeo, & Moore, 2015). A subset of this category – and one of interest in this study – is involved in translational masking and is composed of a relative handful of proteins, including FRGY2A/B, xCIRP2 (Matsumoto et al, 2000), Xtr (Mostafa et al, 2009), Xp54and CK2α (Weston and Somerville, 2006), and B23/nucleophosmin (Singh, Pratt & Yeo, 2015).

Describing all of the types of mRNP is a Herculean task. mRNP complexes have a variety of functions, from cell cycle regulation, to stress response, to mRNA shuttling and degradation (Singh, Pratt, Yeo, & Moore, 2015). It is unsurprising that the components of the mRNP are similarly diverse, with proteomic analyses identifying around 800 possible participants (Baltz et al, 2012).

Following the same theme, mRNP regulation is a complex affair. mRNPs have been observed to repress translation with the DExD/H box ATPase, but unlike FRGY-mediated translational masking, appears to lead to mRNA degradation (Carroll, Munchel, and Weis, 2011). The literature is likewise full of evidence demonstrating the regulatory role of an extensive list of other mRNA-binding or -associated proteins, as well as modification of mRNA and the activity and progression of other processes around transcription and translation (Singh, Yeoh, Pratt & Moore, 2015).

Of primary interest here is the ability of FRGY-based mRNPs to regulate translation through masking and nucleolar disassembly. One important factor of

nucleolar mRNP formation and translational masking is FRGY2, which binds mRNA and is responsible for forming a compact mRNP (Matsumoto et al, 2003). This project will also focus on one component of the mRNP complex: FRGY2A1/2 (previously known collectively as mRNP4), and FRGY2B (previously known as mRNP3) (Deschamps, Viel, Garrigos, Denis, & le Maire, 1992).

mRNA Binding

FRGY is a member of the Y-Box protein family. Structurally, it resembles the archetypal Y-box protein. It contains a well-characterized 5-stranded, β-barrel, cold shock domain (CSD) and RNA binding motif. Its C-terminal region is composed of alternating groups of basic and acidic amino acids, and contains an RNA binding motif (Matsumoto & Bay, 2005). As DNA binding proteins, they recognize the Y-Box sequence and act as a transcription factor, increasing overall gene expression (Matsumoto & Wolffe, 1998). (Figure S1).

In addition to acting as a transcription factor, the protein itself also exhibits two forms of mRNA-binding ability. It has been shown that the CSD binds to mRNA in a sequence-specific manner, while the C-terminal binding domain interacts in a nonspecific fashion. In addition, the target of the CSD has been identified as a 6-nucleotide consensus sequence. (Bouvet, Matsumoto, & Wolffe, 1995).

As mentioned earlier, the three isoforms of FRGY2: FRGY2A1, FRGY2A2, and FRGY2B share most of their sequence. FRGY2A1 and FRGY2A2 differ at the C-terminus, in a region of the protein responsible for several functions, including nonspecific RNA binding, DNA binding, and nuclear localization, among others (Figure S1). At the N-terminal end of the protein, FRGY2A1 and FRGY2A2 are identical to one another, but differ from FRGY2B. All FRGY2A/B forms have an identical cold shock domain, which determines sequence-specific mRNA binding, though other FRGY proteins (such as the somatic form FRGY1) exhibit some differences in amino acid sequence (Figure S2).

Of these three domains – the C-terminus, N-terminus, and CSD – I will focus on the latter two. While the C-terminal domain exhibits interesting mRNA behavior, it is fragile and difficult to work with. The CSD possesses known RNA-binding properties, while the N-terminus is likely involved in certain protein-protein interactions .

Translational Masking

In addition to being an RNA binding protein, FRGY2 also serves as a translational repressor, preventing maternal mRNA from being translated in frog oocytes (Ranjan, Tafuri, & Wolffe, 1993). While the CSD is necessary for FRGY2A/B inclusion in the mRNP complex, it does not appear to be required for translational silencing; this can be accomplished in vitro by the C-terminal

domain by itself (Matsumoto, Meric & Wolfe, 1996). It appears as though the C-terminal and CSD domains may have a cooperative effect, wherein the CSD binds with sequence-specificity, and the C-terminal domain inhibits translation (Bouvet, Matsumoto, & Wolffe, 1995).

The actual mechanism of translational masking is a complex one. Low levels of FRGY can increase translation, whereas larger levels inhibit it. At low concentrations, Y-box proteins may destabilize the secondary structure of mRNA, allowing translation (Matsumoto & Wolffe, 1998). At higher concentrations, as mentioned earlier FRGY has the opposite effect, prompting the disassembly of the nucleolus and a blanket cessation of all translation. FRGY2A/B also acts through a much more targeted method, with the cold shock domain binding to a specific sequence as mentioned earlier. The different mechanisms of action may in part be due associations between FRGY and other mRNP components in a dose-dependent fashion. Alternatively, it could be caused by the basic "math" of translation – while transcription factors affect DNA (typically at low- or single-copy numbers), translation maskers must bind and suppress many copies of mRNA to produce a noticeable effect.

As with mRNA binding, the ability of FRGY2A/B to mask mRNA and inhibit translation has only been studied as a whole, albeit with many experiments describing the effect of particular domains of FRGY2A/B on translation without regards to a specific isoform. This work can be expanded upon and refined using a combination of isoform-specific FRGY2A/B constructs, and a much more

consistent environment in the form of an *in vitro* transcription and translation system, supplied by Promega.

Nucleolar Dynamics

The nucleolus is a non-membrane bound organelle and its structure of the nucleolus is surprisingly complex and dynamic (Lam & Trinkle-Mulcahy, 2015). The mechanisms driving this complexity involve interactions between several different proteins, mRNA, rRNA, miRNA, RNA polymerase, and specific regions of chromatin, all actively bound together (in an ATP-dependent manner) into a hydrogel droplet. Structurally, the nucleolus is separated into the fibrillary center (FC), which sequesters RNA polymerase, and the dense fibrillary components (DFCs), which contains other processing machinery. The outer and final layer is the granular component (GC). It appears as though transcription occurs at the FC/DFC interface, while rRNA processing and ribosome assembly occur in the GC.

As a small, non-membrane bound organelle, the nucleolus is suited to repeated and rapid assembly/disassembly cycles. In prophase, transcription tapers off and ceases as nucleolar proteins dissociate and disperse throughout the nucleus. The regulation of the RNP within the nucleolus appears to be an actively regulated process, possibly tied to the cell cycle; FRET imaging shows that RNP components fibrillarin, Bop1, Nop52, and nucleophosmin/B23 are often co-

localized following nucleolar disassembly, but do not actually interact with one another (Hernandez-Verdun, 2011).

In a pair of related papers, Gonda et al. demonstrate that the C-terminal domain of FRGY2a is able to trigger nucleolar disassembly (Gonda, et al., 2003) and that this activity is dependent on the presence of the nucleolar protein B23 (Gonda, et al., 2006). They postulate that disassembly is triggered by FGRY2a binding and sequestration of B23. However, in an earlier paper, it was shown that B23 RNA binding activity is tightly regulated by phosphorylation by Cyclin B/cdc2, which is in turn, coupled with the cell cycle (Okuwaki, Tsujimoto, & Nagata, 2002). This suggests that regulation of nucleolar disassembly may involve joint control over component availability and activity, or that FRGY2a is involved in B23 phosphorylation, as direct interaction between the two was also observed through co-immunoprecipitation by Gonda et al. Other research shows that FRGY2 associates with (though does not necessarily directly interact with) Xtr, which is in turn, a driver of karyogenesis (Mostafa, et al., 2009). This adds further evidence to the involvement of FRGY2 in the cell cycle.

FRGY2A/B and Disease

As important participants in mRNA binding and translation, Y-Box proteins are associated with many diseases. Aberrant post-translation modification of Y-box protein YBX1, for example, is associated with several forms of cancer (Prabhu, et al., 2015). Likewise, YBX2 (an FRGY2 ortholog) and YBX3 are

critical to spermatogenesis – knocking out one of these genes dramatically reduces fertility, while double knockout results in complete infertility (Snyder, et al., 2015). Given their presence in the nucleolus, and their role in nucleolar disassembly, nonfunctional or malfunctioning mRNP components can also disrupt proper functioning of the nucleolus.

In a more general sense, nucleolar abnormalities are present in most cancer cells. The presence of numerous, large nucleoli in cancer cells has been observed as far back as 1936 (McCarty, 1936). As the nucleolus is the site of ribosome assembly, a hyperactive and rapidly-dividing cell would require several to sustain the increased demand for translation and protein production. In fact, nucleoli may contribute to the malignancy of cancer when nucleolar stress pathways are "broken" and increasingly abnormal expression patterns go unchecked (Quin, et al., 2014).

In turn, nucleolar function feeds into other pathways. Deficiencies in ribosome assembly are known to result in nucleolar stress, which results in free ribosomal subunits. This overloads ubiquitination and proteasomal degradation, causing a buildup of p53, and important tumor suppressor (Zhang & Lu, 2009). The resulting halt in the cell cycle and subsequent apoptosis has been implicated in several neurodegenerative diseases (Tsoi & Chan, 2013).

These are just a few general examples of the importance of proper nucleolar function to the smooth running of the cell. Given FRGY's intimate role in nucleolar function, as well as its ability to initiate nucleolar disassembly, it may

have clinical relevance to malignant cancers and certain neurodegenerative diseases.

Chapter II

Materials & Methods

Design of C-Terminal His-Tagged FRGY2A/B Constructs

FRGY2A/B isoforms were amplified and inserted into the 6-His tagged protein expression vector, pET301-CT-His. The tagged proteins were purified by FPLC on a nickel affinity column. (Figure S3).

More specifically, FRGY2A1, FRGY2A2, and FRGY2B DNA sequences were PCR amplified using custom-made templates purchased from Integrated DNA Technologies, based upon sequences from X. laevis. Primers introduced restriction sites (XbaI and XhoI) at the ends of the amplified product. (Table 1)

Resulting amplified DNA was inserted into pCR2.1, using TOPO™ TA Cloning™ kit (Thermo Fisher Scientific), cloned, and verified by sequencing. Successful clones were isolated, expanded, and plasmids purified by Miniprep™ (Qiagen). Purified plasmid was digested with XbaI and XhoI restriction enzymes and the fragment containing FRGY2A/B ("insert") isolated by gel electrophoresis and purified by gel extraction. Purified FRGY2A/B insert was combined with XbaI- and XhoI-digested and gel pET303-CT-His ("vector"). Vector and insert were combined at a 1:3 ratio, concentrated by glycogen DNA precipitation. Precipitation was performed by addition of 20µg Glycogen, 5µl 3M sodium acetate, and 50µl isopropanol. Following overnight incubation at -20°C, one wash

with 70% ethanol, and 45min of drying, pellet was resuspended in water, and treated with T4 DNA ligase.

FRGY/pET303-CT-His plasmid was transformed into TOP10™ cells (Thermo Fisher Scientific), cloned, and sequenced to verify the absence of mutations, proper directionality, and reading frame. Suitable clones were expanded, purified, and transformed into BL21-Star™ (Thermo Fisher Scientific), bacteria optimized for large scale protein expression.

Expression

FRGY2A/B constructs were inoculated from starter culture at mid-log phase into 1L Magic Media™ (Thermo Fisher Scientific) and expressed overnight at 37°C.

Purification

Following overnight expression, cells were pelleted and resuspended in 20ml lysis buffer (PBS, 1% Triton-X100, Protease Inhibitor Cocktail, DNaseI, 20μM B-mercaptoethanol). Resuspended cells were lysed by two passes through a French pressure cell at 20,000psi and clarified by centrifugation at 18000xg for 30min.

Clarified lysate was heat-treated at 80°C for 30min, followed by 30min incubation on ice, and 30min centrifugation at 3000xg. Pellet containing insoluble

proteins was discarded, enriching the supernatant in thermostable tagged-FRGY2A/B proteins.

Heat-treated lysate was introduced to FPLC using BioScale™ Mini Nuvia™ IMAC column containing Ni^{2+} charged resin. Bound protein was washed and eluted using the following program with 50mM NaH_2PO_4 300mM NaCl and varying concentrations of imidazole. (Table 2)

Gel Electrophoresis

SDS-PAGE was performed using Bolt™ gel system (Thermo Fisher Scientific) and 4-12% Bis-Tris gels. Native gels were run using the NativePAGE™ system (Thermo Fisher Scientific).

Western blots were performed using the Bolt™ system and transferred to nitrocellulose (BioRad) with the iBlot™ 2 Gel Transfer Device (Thermo Fisher Scientific). Detection and blot scanning were performed using an Odyssey® Imaging System (Li-Cor Biosciences).

Antibodies

Western blot probing and immunoprecipitation assays were carried out using custom-produced rabbit polyclonal antibodies against synthetic peptides corresponding to amino acid sequences specific to FRGY2A/B isoforms. (Table 3)

Unless otherwise noted, Western blots were stained at a dilution of 1:1000 with anti-FRGY2A1 and anti-FRGY2A2, and 1:500 with anti-FRGY2B.

Immunoprecipitation

Immunoprecipitation assays were performed using specific Rabbit anti-FRGY2A/B antibodies and Protein A agarose beads. To examine interactions between FRGY2A/B isoforms, proteins were combined and incubated at room temperature for 30 minutes, and then subsequently incubated with beads that had been pre-bound with 4μg of relevant antibodies. Co-incubation was carried out in Nucleolar Lysis Buffer: 142.7mM NaCl, 4.5mM KCl, 2mM MOPS, 2.5mM $MgSO_4$, pH 7.4 (Vandelaer, Thiry & Goessens, 1996). As it is formulated to recover intact nucleoli during cell lysis and fractionation, it provides as close to physiological conditions for nucleoli as reasonably possible.

Following repeated washes, beads were resuspended in SDS sample buffer and boiled. After brief centrifugation, Western blot was performed directly on the supernatant.

Phosphate-modification and mass spectrometry

Phosphorylation was performed with Casein Kinase 2 (CK2) (New England Biolabs, P6010) and 10x NEB Kinase Buffer. Phosphate was provided by ATP disodium salt solution (100mM, pH7) (Sigma, A6559). Approximately

5µg of protein was combined with 20units of CK2 and and 20µM ATP in 1x NEB Kinase Buffer/water and incubated at 30°C overnight.

Dephosphorylation was accomplished with Calf Intestinal Phosphatase (CIP) (New England Biolabs, M0290). Approximately 5µg of protein was combined with 1 unit of CIP in 1xCutSmart buffer and incubated at 37°C for 30min.

Protein was prepared for mass spectrometry by running on SDS-Page gel (8% Bolt gel, Thermo Fisher). After Coomassie staining and thorough washing with HPLC-grade ultrapure water in an unused container, bands were carefully excised such that no unstained gel was included. Gel slices were washed twice in HPLC-grade water with 50% acetonitrile. Gel slices were then frozen at -20°C until needed. Throughout, special care was taken to thoroughly wash instruments and surfaces with HPLC-grade water, use new/unused containers, and prevent contamination by keratin or other proteins in the environment. Mass spectrometry was carried out by the Harvard University Northwest Laboratory Core Facility.

Crosslinking

Prior to crosslinking, protein was dialyzed against crosslinking buffer (20mM NaH_2PO_4, 150mM NaCl, pH8) for several hours to fully exchange buffer. Crosslinking was carried out by combining approximately 2µg of protein with varying concentrations of DMP (diluted from a freshly-prepared stock of 10mM DMP) and incubating at room temperature for 1hr. Reaction was stopped by

addition of Tris-HCl, pH7 to a final concentration of 50mM. In the case of SDS-PAGE/Western blot, crosslinked protein was not boiled, but rather incubated in 1x SDS sample buffer for 1hr at room temperature to preserve crosslinking.

In vitro Transcription and Translation

For functional expression and translational silencing experiments, FRGY2A/B isoforms were expressed using an *in vitro* transcription/translation system, also known as a Rapid Translation System (RTS). This process used the E. coli T7 S30 Extract System for Circular DNA (Promega, #L1130). For FRGY2A/B expression, the template was FRGY2A1, FRGY2A2, or FRGY2B cloned into pCR3.1 containing an upstream T7 promoter site, via TOPO™ TA kit (Thermo Fisher Scientific). For GST reporter expression, the template was GST in pCR3.1 containing an upstream T7 promoter site. Reactions used 10µg of template were carried out on a shaker at overnight at 30°C.

For experiments involving protein-protein interactions a variant mammalian-derived cell-free expression RTS kit was used, referred to here as "Mammalian RTS". These experiments used the TnT® Quick Coupled Transcription/Translation Kit (Promega #L1170). The Mammalian RTS system used the same templates and reaction conditions as the RTS system.

Translational silencing assays used a two-stage RTS protocol. In the first stage, reaction mixes were assembled as per standard protocol using specific

FRGY2A/B templates and were expressed at 30ºC for 2 hours. Second stage reactions were assembled with a modified reaction mix consisting of T7 S30 *E. coli* extract, S30 Premix, complete amino acid mix, GST reporter plasmid, and the product from stage 1 (expressed FRGY2A/B) or combinations of stage 1 reactions. Reactions resumed at 30°C for an additional 10 hours.

Translational silencing assays were also performed substituting the first stage RTS with FPLC-purified FRGY2A/B. These reactions were assembled with a modified reaction mix consisting of T7 S30 *E. coli* extract, S30 Premix, complete amino acid mix, GST reporter plasmid, with the remainder of the volume (9µl in a standard 50µl reaction) composed of FPLC-purified FRGY2A/B . Reactions were carried out on a shaker at 30°C for only 30-60 minutes to avoid running the RTS reaction to depletion and risk losing possible translational silencing effects from FRGY2A/B.

To improve the signal/noise ratio of the reaction, expressed GST reporter was purified by the addition of 2 reaction volumes glutathione agarose beads (Pierce) and 5reaction volumes of PBS to the completed reaction mix (e.g. 100µl bead slurry and 250µl PBS to 50µl RTS reaction). The mix was incubated for 1hr at room temperature on a rocker, followed by centrifugation at ~20,000g for 2 minutes and several washes with PBS/0.5% Tween-20. Special care was taken to avoid loss of beads during washed. GST-bound beads were resuspended in SDS sample buffer, boiled, and briefly centrifuged. Supernatant was used for analysis by SDS-PAGE followed by Coomassie staining or Western blot.

Chapter III

Results

Interaction of FRGY2A/B

A major aim of this project is to investigate the interaction of FRGY2A/B isoforms with both themselves and others. As described previously, all FRGY2A/B forms possess an RNA binding domain at the C-terminus, and the N-terminal domain seems to be involved in protein-protein interactions.

FPLC Purification

The earliest indication of possible self-association was present after FPLC purification. When purifying E. coli-expressed FRGY2A/B-CT-His by Ni-NTA FPLC, multiple peaks were present in the A280 trace. (Figure 1) Each peak appeared consistently 1 column volume (CV) after a stepwise increase in imidazole in the elution buffer. The identity of the protein(s) present in each peak was determined by SDS-PAGE (Figure 2). The same protein (FRGY2A1 in figure 2) is present in each peak in association with a moderate amount of contaminants or breakdown products noticeable in peak 1.

The possibility remained that the pattern of peaks and bands were an artifact of the expression or pre-FPLC purification. The heat treatment step in particular, introduced the possibility of microaggregate formation or other

anomalous interactions among FRGY2A/B during denaturation and refolding. Omission of the heat treatment step in the purification protocol reduced the FRGY2A/B yield but did not affect the pattern of bands on SDS-PAGE (data not shown)

The distribution of FRGY2A/B into multiple peaks could suggest that these proteins form homopolymers. This hypothesis was investigated with dimethyl pimelimidate (DMP) crosslinking. Consistent with previous experiments, increasing concentration of DMP corresponded with increased intensity of higher-mass bands on Western blot. (Figure 3) Interestingly though, the number of low electrophoretic mobility products corresponding to cross-linked proteins increases from Peak 2 to Peak 5. This suggests that crosslinking of larger complexes occurs more readily in later peaks.

Following up on the crosslinking experiments, and the suggestion that later peaks contained complexes or aggregations of FRGY2A/B, I went back to the output of the FPLC purification. Was it forming stable complexes, or was interaction an artifact of purified, concentrated protein? To address this, I performed sequential FPLC. Upon completion of a first round of FPLC purification from heat-treated cell lysate, I immediately re-injected the fractions corresponding to Peak 2 and ran the program again, using a new Ni-NTA column. (Figure 4) The process was repeated with Peak 5 from the first round. Side-by-side gel and staining shows a very slight upward shift in high-intensity bands with respect to fraction number. This shift does not extend to a shift in overall peak intensity, and may represent simple variation between runs. Re-injection of Peak

5 does not demonstrate an enrichment in later peaks as would be expected from a strong self-interaction in purified FRGY2B.

Another method to assess self-assembly was to analyze peaks by native gel electrophoresis, which would preserve protein complexes. Native gels of previous rounds of purification have consistently resulted in 5 bands ranging from 28-98kDa, all of which stain positive for the appropriate FRGY2A/B on Western blot. Re-purification was performed again with re-injection of Peak 2 from FRGY2A2, and once again the content of Peak 2 was distributed between multiple peaks which were analyzed by native gel electrophoresis. The distribution and relative intensity of the bands were compared between peaks. (Figure 5) Relative intensity of the bands is shown as a percentage of that peak's total intensity (all bands in all of that peak's fractions) in to compensate for the fact that the total amount of protein varies between fractions and peaks. The data shows that, from peak to peak, there is no practically significant difference in the distribution of protein between the 5 bands.

Nucleic Acid Binding

E. coli possesses similar cold-shock proteins and sequence domains of its own (Graumann, 1998), so the possibility existed that interactions between FRGY2A/B had bound to bacterial DNA or RNA during expression. Following heat treatment, FRGY2A1-CT-His lysate was treated with DNase and RNase, and

purified by FPLC. (Figure 6) Distribution of protein among the resulting fractions remained unchanged, suggesting that in this situation, nucleic acid binding does not play a significant role in either protein solubility or the observed self-interaction.

Antibody Characterization

To effectively detect FRGY2A/B and distinguish its specific isoforms, we purchased custom-produced polyclonal antibodies raised against synthetic peptides specific to individual FRGY2A/B isoforms. To test the efficacy of these antibodies, as well as their specificity, a Western blot was performed on FPLC-purified FRGY2A/B (Figure 7). By co-staining with antibodies against the His-tag present in all three constructs, a comparison between stained FRGY2A/B and total FRGY2A/B could be made. All three antibodies showed good levels of staining and acceptable specificity, with only minor cross-reactivity. In practice, the FRGY2B antibody proved to be the most temperamental, though sensitivity issues were largely resolved by increasing the concentration of antibody when staining, and by increasing the incubation time.

Co-Immunoprecipitation

To more directly examine possible interactions between different FRGY2A/B isoforms, a series of co-immunoprecipitations was performed. Pulldown of purified FRGY2A1 co-incubated with FRGY2A2 and FRGY2B showed possible interactions (Figure 8).

Initial experiments showed high levels of nonspecific binding, which was reduced after adjusting the protocol to include pre-binding of the pulldown antibody with Protein A agarose beads, in addition to blocking with BSA. Some level of nonspecific binding remained, possibly due to limitations of the available antibodies, which were all shared "rabbit" as their host species. Several lanes, however, show a distinct increase in signal, suggesting that FRGY2A2 was pulled down with FRGY2A1 (data not shown).

To verify the previous results, a reciprocal coIP was performed, using FRGY2A2 as the pulldown antibody (Figure 9). This experiment likewise suggests that FRGY2A1 and FRGY2A2 interact, since FRGY2A1 precipitates with FRGY2A2 when pulled down, but does not appear in large amounts in the absence of FRGY2A2. As yet, it is unclear whether FRGY2B interacts with FRGY2A1 and FRGY2A2, as the signal was not significantly different from the nonspecific binding in the control lane. Inconsistent efficacy of the FRGY2B

antibody has been a problem in the past, though, so interaction cannot be ruled out.

Phosphorylation / Mass Spec

Based on amino acid sequence, FRGY2A/B isoforms possess multiple potential phosphorylation sites. This provided an avenue of investigation as to one of FRGY2A/B's functions: translational silencing. To verify actual phosphorylation, we treated FPLC-purified FRGY2A1 and FRGY2A2 with casein kinase 2 (CK2). In the absence of antibodies specific to phospho-FRGY2A/B, we relied on gel shift. On SDS-PAGE, we observed a slight upwards shift in both FRGY2A1 and FRGY2A2 when treated with CK2. (Figure 10)

For a more precise look at phosphorylation of FRGY2A1, purified protein was treated with either kinase or phosphatase and run on SDS-PAGE, as in the previous experiment. This time, the bands were carefully excised, washed, and sent for analysis by mass spectrometry. The results showed a large difference in phosphorylated residues between the phosphatase- and kinase-treated protein. (Figure 11). Not all potential phosphorylation sites were modified following kinase treatment, and six retained their phosphate following phosphatase treatment (Table 4). It should be noted that the kinase-treated FRGY2A1 is likely hyperphosphorylated, containing more modified residues than would likely be present *in vivo*.

To minimize the variables associated with introducing a reporter plasmid and purified FRGY2A/B into a translating system (i.e. cells in culture) we opted to use a Rapid Translation System (RTS) kit for *in vitro* transcription and translation. The reporter plasmid allows for in vitro transcription and translation of with Glutathione S-Transferase (GST). Previous experiments had shown that the FRGY2A/B protein could be expressed to high levels through RTS, then added to a second RTS reaction containing the GST reporter. Such sequential RTS resulted in decreased expression of GST, indicating translational silencing (data not shown).

Using a similar approach, we examined the effects of phosphate-modified FRGY2A1 and FRGY2A2 on transcription within the RTS model. (Figure 12) In these experiments, we used FPLC-purified FRGY2A1/2 both to start with a consistent, known amount of FRGY2A1/2, and because the proteins present in the *E. coli* extract of the first-stage RTS reaction could potentially interfere with the initial phosphorylation or dephosphorylation of FRGY2A1/2. Compared to the control, unmodified (A1C, A2C) and CP2-treated FRGY2A1/2 (A1K, A2K) led to a noticeable decrease in GST expression. FRGY2A1/2 that had been dephosphorylated with CIP (A1P, A2P) showed an even more dramatic decrease in GST expression. As a further control, the assay was run by directly adding CP2 (K) or CIP (P) to the reaction mix in the absence of FRGY2A1/2. These conditions did not result in a noticeable change in GST expression compared to controls (C) in which the GST expression was run "clean" without the addition of FRGY2A/B, CP2, or CIP. This suggests that FRGY2A1/2 is able

to silence translation *in vitro*, and that the dephosphorylation of FRGY2A1/2 increases its ability to silence translation.

Chapter IV

Discussion

Protein-Protein Interactions

FPLC purification of His-tagged protein by Ni-NTA column relies on the strong metal affinity of a chain of six histidine residues added to the protein of interest. The protein can then be bound to a column with resin-immobilized Ni^{2+}, and other compounds or contaminating proteins washed out. It is then eluted by the addition of imidazole (the metal-binding side chain of histidine), which out-competes the histidine for available Ni^{2+}, causing the His-tag and protein to be released from the column.

What began as a simple attempt to purify His-tagged FRGY2A/B by FPLC showed hints that the protein self-associates. Purified His-tagged protein should elute from the column in a single, distinct band. Multiple smaller bands could indicate protein degradation or co-purified associated proteins (dissociated by sample preparation for SDS-PAGE), while larger bands could indicate modification of the protein, or interactions with other proteins (when viewed on native gels) (Figure 5).

An intriguing possibility was that FRGY2A/B could self-associate. A key observation was the fact that FRGY2A/B consistently eluted in multiple peaks, each following approximately one column volume after a step-wise increase in imidazole concentration (Figure 1). This hypothetical interaction would result in

dimers, trimers, and tetramers – each additional FRGY2A/B polypeptide in a complex adding an additional His-tag, and thus requiring a higher concentration of imidazole to displace the bound multimer from the resin. This particular behavior does not appear to involve any additional co-purified proteins, as no additional proteins are evident in SDS-PAGE analysis (Figure 2).

While suggestive of FRGY2A/B self-interaction, the observed FPLC results were not conclusive on their own. The possibility remained that interaction could be due to some other factor present in the *E. coli* lysate or inherent to the lysis or purification process. Alternatively, it could be an artifact of the overexpression and concentration of FRGY2A/B; an abnormal interaction due to the artificially high concentration of the protein. Finally, it could be a side-effect of the heat-treatment stage of purification. While ostensibly thermostable, there was a chance the FRGY2A/B could form microaggregates when heat treated in a concentrated solution (unlikely, since the multiple peaks were also present with untreated protein), and lysate was filtered through a 0.2μm syringe filter immediately prior to injection into FPLC system.

Investigation of protein-protein interactions between FRGY2A/B began with DMP crosslinking. Consisting of two active groups connected by a long spacer, DMP will bind covalently to primary amine groups and crosslink proteins that are close enough together. At the proper concentration, it should crosslink proteins that are close enough to be interacting with one another. The findings of this experiment were consistent with this interaction, with larger bands becoming more intense as the concentration of DMP was increased. Peak 5, for example, is

expected to represent a larger complex than Peak 2, given the same concentration of DMP, and should therefore give more cross-linked product with low electrophoretic mobility. This is what was observed (Figure 3). Therefore, I propose that FRGY2A/B is able to self-associate all the way up to a pentameric complex, though the dimer is the most stable based on the consistently-strong Peak 2 in FPLC.

To gauge the strength of these potential interactions, we carried out several two-stage purification experiments. In these experiments, stage one consisted of the FPLC purification of bacterial lysate as described earlier. Following the first stage, fractions corresponding to a given A_{280} peak would be re-injected and run through the column again. The stability of any FRGY2A/B complexes could be roughly estimated from the output of this second stage – a stable complex would result in a relative intensification of the re-injected peak (in the A_{280} trace, and subsequent gel) and a depletion of the other peaks. In contrast, a less stable complex would quickly return to equilibrium, with the purified monomer, dimer, trimer, etc., quickly redistributing into the range of peaks observed in the first stage of purification. The presence of a semi-stable complex was supported by native gel analysis, which resulted in multiple bands corresponding with complexes with different stoichiometries (Figure 5).

Re-running a purified peak resulted in a weaker signal overall as the content of one peak was redistributed into multiple peaks. Relative to each other, the peaks from the re-run and their protein content were not significantly different from stage one purification (Figure 4). In addition, the samples reached the new

equilibrium in a matter of hours and the effect persisted for several days. This suggested that the interaction was semi-stable and could settle into equilibrium quickly. These experiments also lent weight to the idea that these interactions were not the direct result of overexpression and purification, since the input of second-stage purification was necessarily more dilute than the input of the first stage, due to loss of protein to the column and the fact that first stage lysate had been spread out over at least 6 peaks, only one of which would be reinjected.

While FPLC purification and DMP crosslinking support the self-interaction of FRGY2A/B isoforms, we wished to take a more direct look at interactions, particularly those between different isoforms. To do so, we performed co-immunoprecipitation following incubation of different purified FRGY2A/B isoforms with each other. CiIP with anti-FRGY2A1 showed a potential interaction between itself and FRGY2A2 (Figure 8). Reciprocal CoIP with anti-FRGY2A2 showed similar, and much more distinct interactions (Figure 9). The Western blot was complicated by the fact that all anti-FRGY2A/B antibodies available to us were raised in rabbits, and thus led to some cross-reactivity. Despite the high baseline signal, there is noticeable increase in band intensity when FRGY2A1 and FRGY2A2 are present together, suggesting co-precipitation.

Investigation of FRGY2B was unfortunately hampered by the quality of the anti-FRGY2B antibody. While anti-FRGY2A1 and -FRGY2A2 antibodies were effective and specific, even in initial experiments, FRGY2B staining was faint and sometimes inconsistent (Figure 7). In this round of CoIP experiments,

FRGY2B was – if present at all – too faintly stained to be visible above the baseline signal. An alternate approach for future CoIP experiments would be to use proteins with different tags, such as FLAG, HA, or GST. Alternatively, CoIP reactions with two untagged proteins and one His-tagged protein could yield a more distinct signal. The easy availability of commercial antibodies to these tags would also produce a cleaner blot and permit dual staining.

RTS Expression

One of the primary functions of FRGY2A/B is to silence translation in oocytes. Prior studies have focused on silencing in a cell-free Xenopus embryo system. Due to the difficulty of establishing that system, in addition to the variation from batch to batch of expressed and purified protein, we elected to use a different method to investigate translational silencing. Promega's T7 S30 Extract system, or Rapid Translation System (RTS), uses an E. coli extract to perform *in vitro* transcription and translation of a gene cloned into a plasmid and under the control of a T7 promoter.

Prior experiments in the lab had established that a two-stage RTS reaction could act be used to demonstrate translational silencing. Expression of a given isoform of FRGY2A/B for 4 hours would provide a supply of FRGY2A/B protein. That reaction could then be added to a second RTS reaction, using a plasmid for GST as a reporter. Early experiments showed a dose-dependent

decrease in GST expression upon addition of increasing amounts of RTS-expressed FRGY2A/B.

While effective, this assay had some limitations that made modifications necessary. The first round of RTS produced consistent, high levels of FRGY2A/B, but addition of the first reaction to the second was still something of a black box; it consisted of adding the reaction *mix* – template, enzymes, and an unknown quantity of expressed FRGY2A/B protein. To remedy this, replaced the first stage of RTS with FPLC-purified protein. This allowed concentration, quantification, and normalization of the input protein, as well as buffer exchange and protein modification.

The modified silencing assay confirmed prior results, that addition of FRGY2A1 and FRGY2A2 silenced translation, decreasing GST expression. We also modified FRGY2A1/2 by phosphorylation and dephosphorylation. Interestingly, phosphorylation by CK2 had little effect, but dephosphorylation by CIP significantly increased the effectiveness of translational silencing (Figure 12). There appeared to be no significant difference between FRGY2A1 and FRGY2A2 in this respect.

Analysis of CP2- and CIP-treated FRGY2A1 by mass spectrometry showed widespread addition and removal of phosphate groups (Figure 11, Table 4). As mentioned previously, the kinase-treated FRGY2A1 is likely hyperphosphorylated and is not representative of the protein *in vivo*. As such, its behavior with regards to translational masking (rather, its lack thereof) may be an artifact of the kinase treatment.

This observation tentatively suggests that dephosphorylation of FRGY2A1/2 increases its effectiveness due to changes in the protein itself, as opposed to binding or dissociation with accessory proteins. The input in this reaction was purified protein, with negligible amounts of other nucleolar proteins and suspected FRGY2A1/2 binding partners. Further experiments are necessary to come to a more solid conclusion, including CoIP with FRGY2A1/2 and E. coli lysate to determine if any homologs of FRGY2A1/2-associating proteins are endogenously expressed in bacteria. In addition, the silencing assay could be modified to use so-called "Mammalian RTS" - Promega's TnT Quick Coupled Transcription/Translation kit, which is similar but derived from mammalian cell extract. This modification could potentially eliminate some artifacts of the original bacterial RTS.

Conclusions

Results suggest that FRGY2A/B is able to self-associate. This doesn't appear to be an artifact of purification – while transient, formation of dimers, trimers, and tetramers appear to occur in a variety of different conditions. In addition, FRGY2A1 and FRGY2A2 appear to interact; an unsurprising finding, given the fact that their N-terminal domains are identical.

Overall, results show a high level of similarity between the different FRGY2A/B isoforms. This similarity extends to translational silencing activity. FRGY2A1 and FRGY2A2 appear to have similar ability to silence translation,

despite the differences in their C-terminal domains. This ability is also dependent on the protein's phosphorylation state, with dephosphorylation markedly increasing silencing. Multiple phosphorylation sites exist within the N-terminal domain, hinting that protein-protein interactions – even self-interactions – play a role in the activity of FRGY2A1/2.

Future Research

First and foremost, many of these findings should be confirmed against all available FRGY2A/B isoforms. FRGY2B proved frustratingly difficult to purify and detect, and as such, was not always available to test alongside FRGY2A1/2. While the data collected suggests that there is not a significant difference between FRGY2A1, FRGY2A2, and FRGY2B in the areas of cross- and self-interaction, and translational silencing, a closer look may reveal more subtle differences.

In addition to further testing of FRGY2B, testing of the individual domains of all three isoforms could lead to insights into FRGY2A/B function and inter-isoform differences.

Initial experiments showed that FRGY2A/B contains several predicted phosphorylation sites. Treatment with kinase (CK2) confirmed modification at many of these sites through mass spectrometry. So far, we have looked at them in terms of translational silencing, but testing the effects of phosphorylation state on

protein-protein interactions, both in transient complex formation and more substantial CoIP interactions, could provide insights into FRGY2A/B activity.

A weakness of the crosslinking approach is that DMP crosslinks proteins that are in close proximity to one another – presumably at a concentration where the only proteins close enough to consistently crosslink are ones that are interacting with one another. However, it is possible for this method to crosslink proteins that are not interacting, or ones that are only briefly associated. As a potential follow-up, crosslinking could be performed to the *E. coli* lysate prior to FPLC purification to determine whether the distribution of peaks persists or is only seen in purified FRGY2A/B. In addition, a repeat of 2-stage FPLC re-purification using crosslinked protein as an input could help determine whether or not the 5-peak pattern is a result of a mix of monomeric through pentameric FRGY2A/B or an artifact.

Finally, my original intent had been to investigate the effects of FRGY2A/B in nucleolar dynamics. While the data from *in vitro* studies are undoubtedly useful, it must be replicated in living systems – in this case, cells in culture would be an appropriate next step. Introducing FRGY2A/B to cells or to purified nuclei may lead to a better understanding of its behavior under closer-to-physiological conditions, as well more directly functional aspects. Preliminary data suggest that nucleoli can be disassembled in purified nuclei, and can then be quantified by flow cytometry, or that populations of nuclei with assembled or disassembled nucleoli can even enriched by FACS. While this method has not yet been tested with FRGY2A/B, its viability has been shown by treatment of purified

nuclei by Actinomycin D, known to halt transcription and lead to nucleolar dissociation, and dual-staining with allophyocyanin (nuclear) and chromomycin A (nucleolar) (Figure S4). Concurrently, preliminary research has shown that it is possible to introduce FRGY2A/B into nuclei irrespective of phosphorylation state through co-incubation (Figure S5). Together, these demonstrate the feasibility of introducing FRGY2A/B to purified nuclei and quantifying the effect on nucleoli through flow cytometry.

References

Baltz, A., et al. (2012). The mRNA-Bound Proteome and Its Global Occupancy Profile on Protein-Coding Transcripts. Molecular Cell 46, 674-690.

Bouvet, P., Matsumoto, K., & Wolffe, A. (1995). Sequence-specific RNA Recognition by the Xenopus Y-box Proteins. The Journal of Biological Chemistry, 28297-28303.

Buchan, J., (2014) mRNP granules: Assembly, function, and connections with disease. RNA Biology, 11:8, 1019-1030.

Carroll, J., Munchel, S., Weis, K., 2011. The DExD/H box ATPase Dhh1 functions in translational repression, mRNA decay, and processing body dynamics. The Journal of Cell Biology, Vol.194, No.4, 527-537.

Deschamps, S., Viel, A., Garrigos, M., Denis, H., & le Maire, M. (1992). mRNP4, a Major mRNA-binding Protein from Xenopus Oocytes Is Identical to Transcription Factor FRG Y2. The Journal of Biological Chemistry, 13799-13802.

Dreyfuss, G. (1986). Structure and Function of Nuclear and Cytoplasmic Ribonucleoprotein Particles. Annual Review Cell Biology, 459-498.

Gonda, K., Fowler, J., Katoku-Kikyo, N., Haroldson, J., Wudel, J., & Kikyo, N. (2003). Reversible disassembly of somatic nucleoli by the germ cell proteins FRGY2a and FRGY2b. *Nature Cell Biology*, 205-210.

Gonda, K., Wudel, J., Nelson, D., Katoku-Kikyo, N., Reed, P., Tamada, H., et al. (2006). Requirement of the Protein B23 for Nucleolar Disassembly Induced by the FRGY2a Family Proteins. The Journal of Biological Chemistry, 8153-8160.

Graumann, P., Marahiel, M. (1998). A superfamily of proteins that contain the cold-shock domain. Trends Biochem. Sci., (8): 286-290.

Hernandez-Verdun, D. (2011). Assembly and disassembly of the nucleolus during the cell cycle. Nucleus, 189-194.

Lam, Y., & Trinkle-Mulcahy, L. (2015). New insignts into nucleolar structure and function. F1000 Prime Reports.

Matsumoto, K., & Bay, B. (2005). Significance of the Y-Box proteins in human cancers. Journal of Molecular and Genetic Medicine, 11-17.

Matsumoto, K. Meric, F. & Wolffe, A. (1996) Translational Repression Dependent on the Interaction of the Xenopus Y-Box Protein FRGY2 with mRNA. The Journal of Biological Chemistry, Vol. 271, No. 37, 22706-22712.

Matsumoto, K., & Wolffe, A. (1998). Gene regulation by Y-box proteins: coupling control of transcription and translation. Trends in Cell Biology, 318-323.

Matsumoto, K. et al. (2000). CIRP2, a major cytoplasmic RNA-binding protein in Xenopus oocytes. Nucleic Acids Research, 29(23), 4689-4697.

Matsumoto, K., Tanaka K., Aoki K., et al. (2003). Visualization of the reconstituted FRGY2-mRNA complexes by electron microscopy. Biochemical and Biophysical Research Communications, 306, 53-58.

McCarty, W. (1936). The value of the macro nucleus in the cancer problem. American Journal of Cancer, 529-536.

Mostafa, G., Sugimoto, T., Hiyoshi, M., Kawasaki, H., Kubo, H., Matsumoto, K., et al. (2009). Xtr, a plural Tudor domain-contatining protein, coexists with FRGY2 in both cytoplasmic mRNP particle and germ plasm in Xenopus embryo: Its possible role in transaltional regulation of maternal mRNAs. The Japanese Society of Developmental Biologists, 595-605.

Okuwaki, M., Tsujimoto, M., & Nagata, K. (2002). The RNA Binding Activity of a Ribosome Biogenesis Factor, Nucleophosmin/B23, Is Modulated by Phosphorylation with a Cell Cycle-dependent Kinase and by Association with Its Subtype. Molecular Biology of the Cell, 2016-2030.

Prabhu, L., Hartley, A., Martin, M., Warsame, F., Sun, E., & Lu, T. (2015). Role of post-translational modification of the Y box binding protein 1 in human cancers. Genes & Diseases, 240-246.

Quin, J., Devlin, J., Cameron, D., Hannan, K., Pearson, R., & Hannan, R. (2014). Targeting the nucleolus for cancer intervention. Biochimica et Biophyisica Acta, 802-816.

Sheth, U., Pitt, J., Dennis, S., Priess, J. (2010). Perinuclear P granules are the principal sites of mRNA export in adult *C. elegans* germ cells. Development, 137(8): 1305-1314.

Singh, G., Pratt, G., Yeo, G., & Moore, M. (2015). The Clothes Make the mRNA: Past and Present Trends in mRNP Fashion. Annual Review Biochem, 325-354.

Snyder, E., Soundararajan, R., Sharma, M., Dearth, A., Smith, B., & Braun, R. (2015). Compound Heterozygosity for Y Box Proteins Causes Sterility Due to Loss of Translational Repression. PLOS Genetics.

Sommerville, J., & Ladomery, M. (1996). Masking of mRNA by Y-Box Proteins. The FASEB Journal, Vol10., No.4, 435-443.

Weston, A., and Sommerville, J. (2006). Xp54 and related (DDX6-like) RNA helicases: roles in messenger RNP assembly, translation regulation and RNA degradation. Nucleic Acids Research, Vol.34, No.10.

Zhang, Y., & Lu, H. (2009). Signaling to p53: Ribosomal Proteins Find Their Way. Cancer Cell, 369-377.

Appendix I

Tables

Table 1: Primer sequences for construction of FRGY2A/B plasmids.

Primer	Sequence (5'-3')
FRGY2A1 Forward	GGGTCTAGAATGAGTGAGGCGGAAGCCCAGGAGCCC
FRGY2A1 Reverse	CCCCTCGAGTTCTGGGGCAGGTGTATCTGAAATCCC
FRGY2A2 Forward	GGGTCTAGAATGAGTGAGGCGGAAGCCCAGGAGCCC
FRGY2A2 Reverse	CCCCTCGAGTTGCAGTGTCCCAAAAATTCCCATGG
FRGY2B Forward	GGGTCTAGAATGAGTGAGGCGGAACCCCGAGAGACTGAAGCGG
FRGY2B Reverse	CCCCTCGAGTTCTGGGGCAGTTGTATCCTCCACTCCTGC

Table 2: Steps for Ni^{2+}-column FPLC purification of His-tagged FRGY2A/B.

	Step	Volume (CV)	Imidazole Conc.
1	Equilibrate	1	20μM
2	Sample App	6	-
3	Wash 1	6	20μM
4	Wash 2	5	50μM
5	Elution 1	5	100μM
6	Elution 2	5	150μM
7	Elution 3	5	200μM
8	Elution 4	5	300μM
9	Elution 5	5	500μM
10	Wash	5	0μM

Table 3: Antibody information.

Target	Manufacturer	Host Species	Target Peptide
FRGY2A1	Genscript	Rabbit	DGAPVQSSAPDPGIADTPAPE
FRGY2A2	Thermo Fisher	Rabbit	VPALFHLPAALDSMGIFGTLQ
FRGY2B	Genscript	Rabbit	EAVTQPEPAPEIHKPDIVPP

Table 4. Mass spectrometry analysis of FRGY2A2 treated with phosphatase (CIP) and kinase (CK2), compared to potential phosphorylation sites. “Yes” and “no” denote the presence or absence of a phosphate at that residue. Credit: Alain Viel, 2019

AA/Position in FRGY2A1	CIP	CK2
Ser 2	Yes	Yes
Ser 17	Yes	Yes
Thr 40	No	Yes
Ser 85	Yes	Yes
Thr 91	Yes	Yes
Thr 109	No	Yes
Ser 119	No	Yes
Thr 199	No	Yes
Ser 202	No	Yes
Thr 211	No	Yes
Ser 212	No	Yes
Ser 217	No	Yes
Thr 246	No	Yes
Thr 254	No	Yes
Ser 258	No	Yes
Thr 284	No	Yes
Thr 289	No	Yes
Thr 299	No	Yes
Ser 304	Yes	Yes
T308	Yes	No

Appendix II

Figures

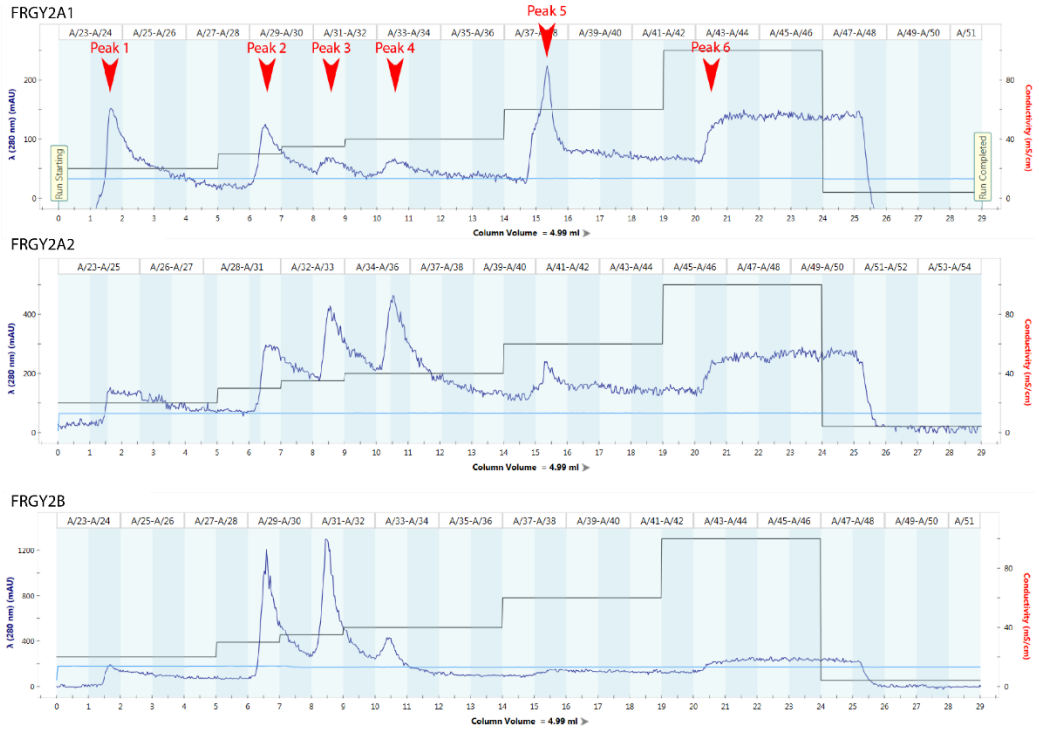


Figure 1. System traces of FRGY2A/B purification by FPLC. Dark blue line indicates A280 of column flow-through. Black line represents concentration of elution buffer (containing imidazole). Light blue line indicates system pressure.

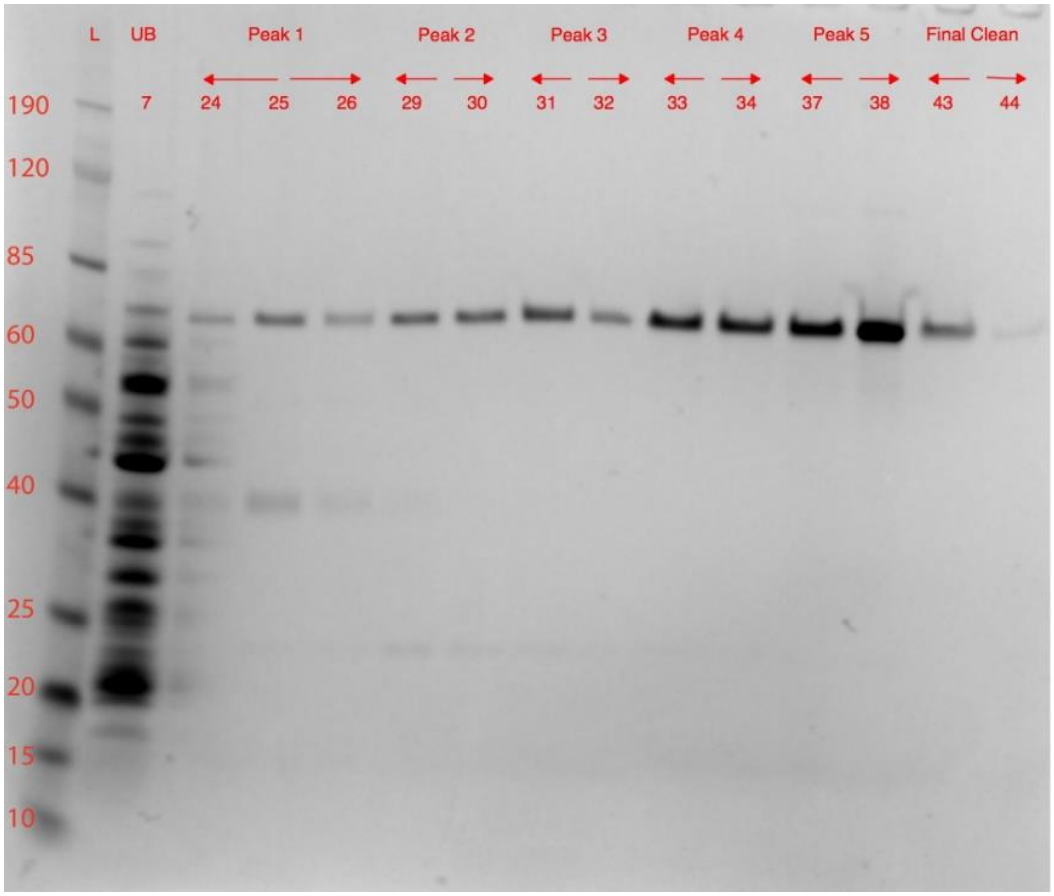


Figure 2. SDS-PAGE and Coomassie staining of FPLC fractions containing eluted FRGY2A1-CT-His. “Final clean” lanes are equivalent to the first two fractions of Peak 6.

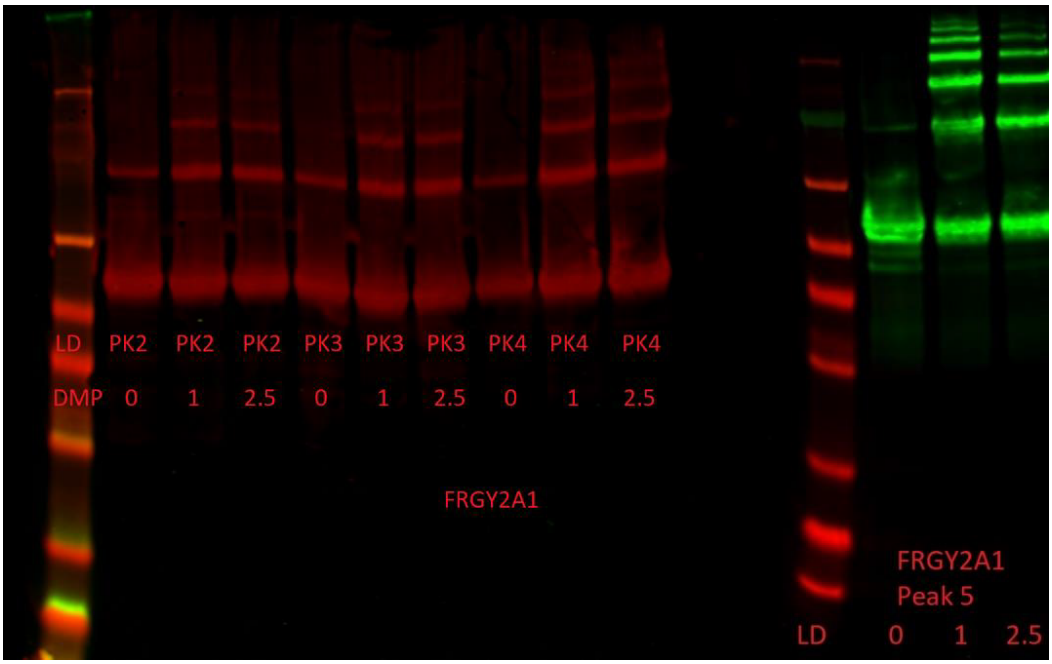


Figure 3. DMP crosslinking of purified FRGY2A1. PK2-5 indicates FPLC peaks 2-5. Numbers indicate DMP concentration (mM). Western Blot.

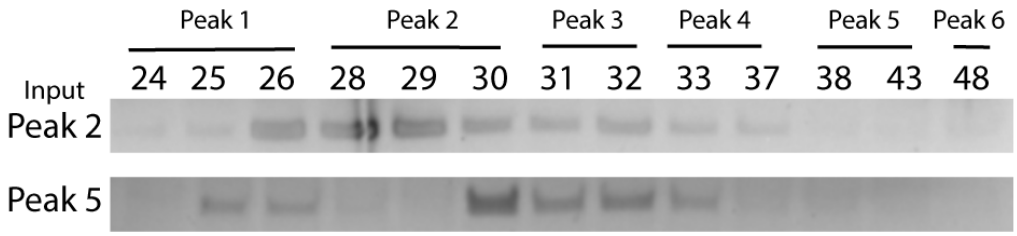


Figure 4. Second-stage FPLC re-run of FRGY2B Peak 2 and Peak 5. Input denotes the pooled fractions of Peak 2 or Peak 5 of first-stage FPLC-purified protein. Upper numbers indicate the fractions and corresponding A_{280} peaks of second-stage FPLC purification. SDS-PAGE and Coomassie stain.

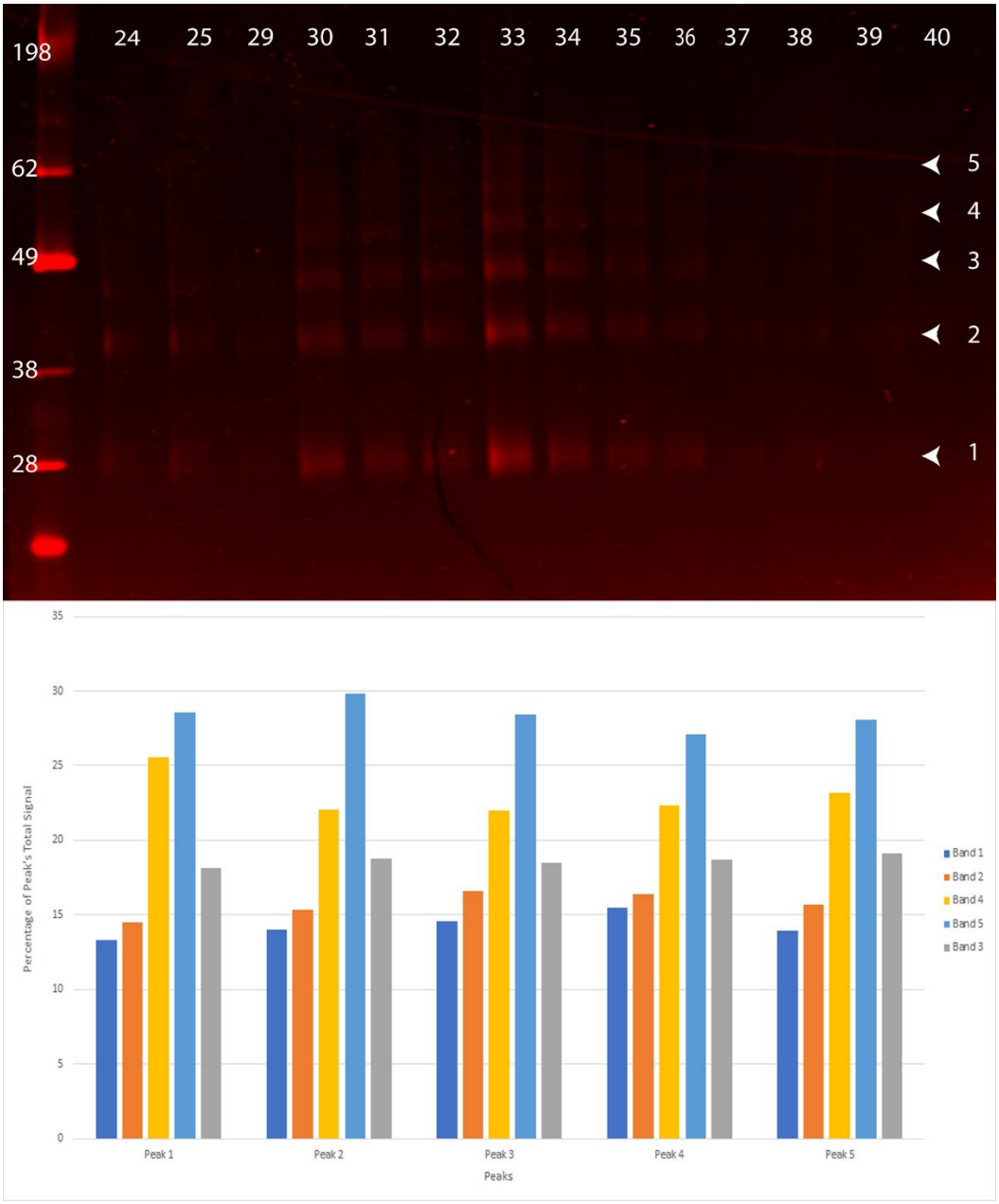


Figure 5. Assessment of stability of FRGY2A2 self-complexing by FPLC re-run of Peak 2 isolated from a prior FRGY2A2 FPLC batch. Top: High-sensitivity scan of Coomassie-stained Native PAGE showing multiple bands in fractions of FPLC-purified FRGY2A2 (Peak1 - Fraction 24, 25. Peak 2 – Fraction 29, 30. Peak 3 – Fraction 31, 32. Peak 4 – Fraction 33, 34. Peak 5 – Fraction 35, 36). Bottom: Percentage total peak intensity of the five common bands produced by Coomassie-stained Native PAGE, by peak.

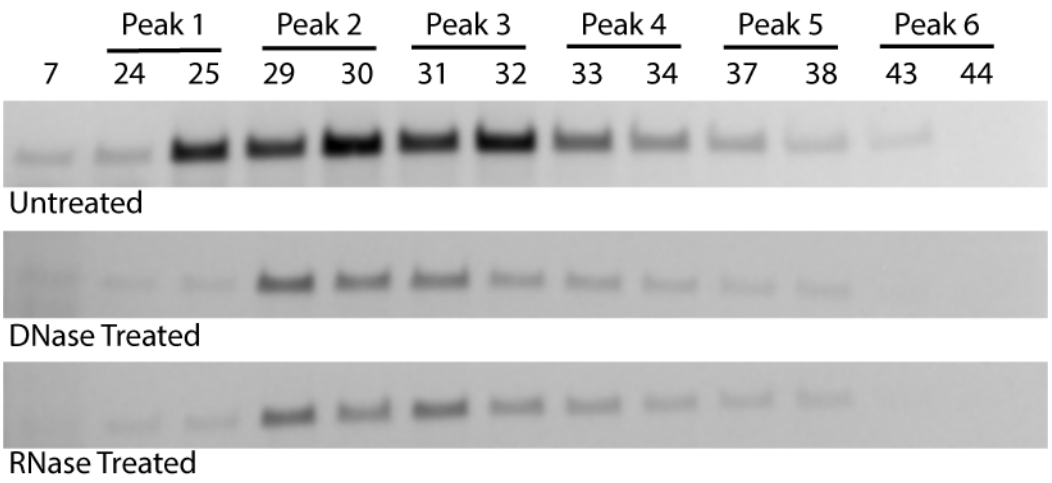


Figure 6. FPLC-purified FRGY2A1-CT-His. Lysate was heat treated as per standard protocol (untreated), treated with DNaseI following heat treatment (DNase Treated), or treated with RNase following heat treatment (RNase Treated). SDS-PAGE and Coomassie stain.

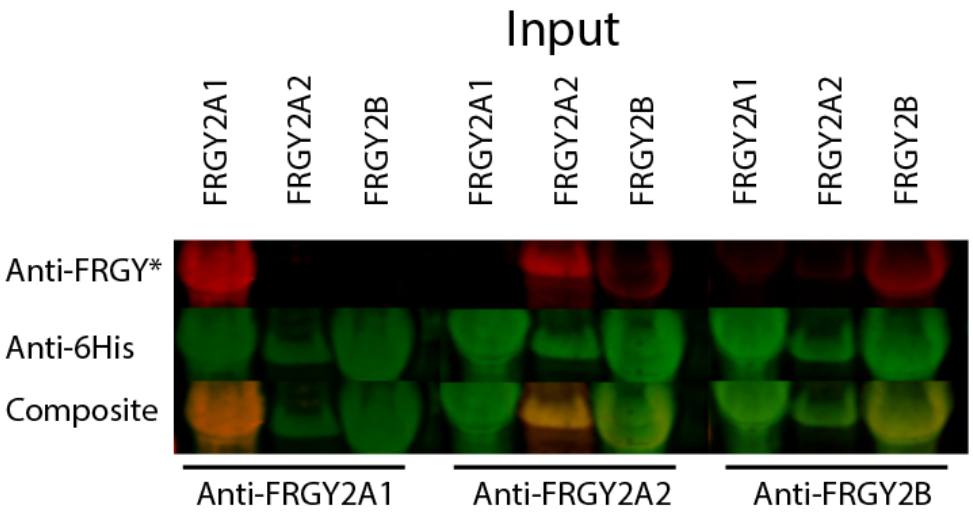


Figure 7. Test of FRGY2A/B antibody sensitivity and specificity. Western blot of His-tagged, FPLC purified FRGY2A/B proteins (upper labels). Dual-stained with antibodies raised against appropriate FRGY2A/B isoform (bottom label) and with antibodies against His-tag.

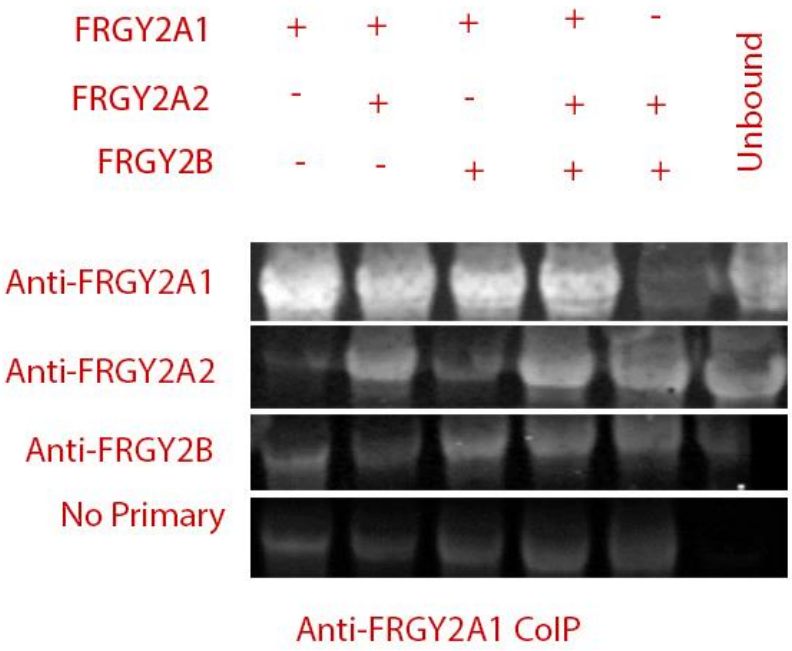


Figure 8. Co-immunoprecipitation with FRGY2A1 of co-incubated, purified FRGY2A/B. Western blot.

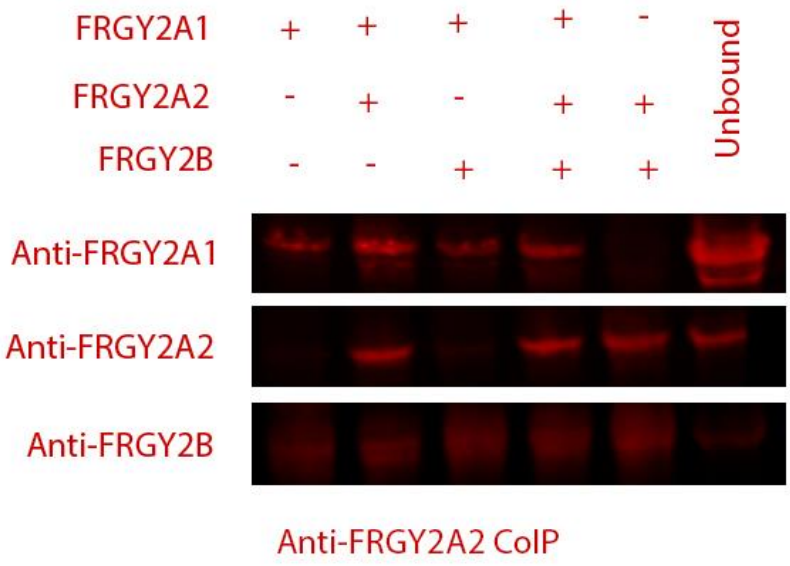


Figure 9. Co-immunoprecipitation with FRGY2A2 of co-incubated, purified FRGY2A/B. Western blot.

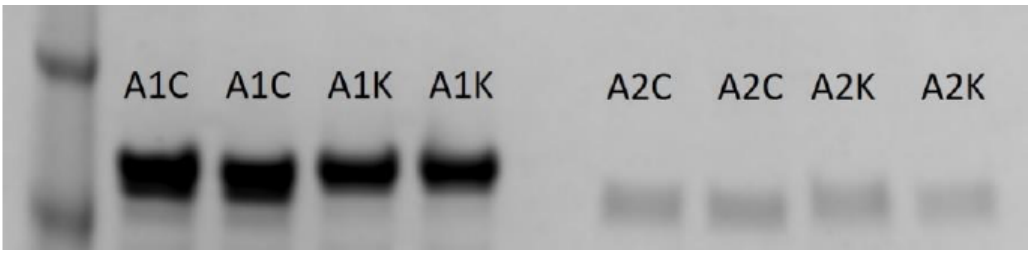


Figure 10. *In vitro* phosphorylation by casein kinase 2 (CK2) of FRGY2A1 and FRGY2A2. *A1C*: FRGY2A1 incubated with water. *A1K*: FRGY2A1 incubated with CK2. *A2C*: FRGY2A2 incubated with water. *A2K*: FRGY2A2 incubated with CK2. Slight upward shift compared to control suggests phosphorylation.



Figure 11. Mass spectrometry analysis of FRGY2A1 treated with CK2 (kinase) and CIP (phosphatase). Green shaded areas denote regions of the peptide covered by the analysis. P denotes a phosphate at a given residue.
Credit: Alain Viel, 2019



Figure 12. Translation inhibition of GST transcription and translation in RTS via phosphate-modified FRGY2A1 and FRGY2A2. *C*: No protein added. *A1C/A2C*: Unmodified FPLC-purified protein. *A1P/A2P*: CIP-treated protein. *A1K/A2K*: CP2-treated protein. *No protein K/P/C*: RTS reaction with only added CP2, CIP, or water, respectively. Western blot against GST.

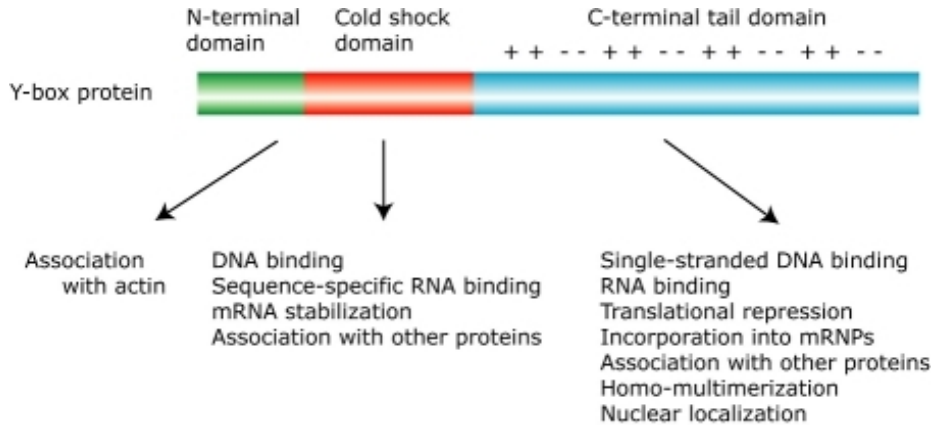


Figure S1. Schematic diagram depicting the structure of the Y-box protein. Matsumoto, K and Bay, B-H. "Significance of the Y-box Proteins in Human Cancers." *J. Molecular and Genetic Medicine*, 1(1), 2005.

```
FRGY1          .....MSSEV ETQQQQPDAL EGKAGQEPAA TVGDKKVIAT KVLGTVKWFN
FRGY2A-1       MSEAEAQEPE PVPQPESEPE IQKPGIAAAR NQANKKVLAT QVQGTVKWFN
FRGY2A-2       MSEAEAQEPE PVPQPESEPE IQKPGIAAAR NQANKKVLAT QVQGTVKWFN
FRGY2B         MSEAEPRETE AVTQPEPAPE IHKPDIVPPR NQINKKLLAT QVQGTVKWFN

FRGY1          VRNGYGFINR NDTKEDVFVH QTAIKKNNPR KYLRSVGDGE TVEFDVVEGE
FRGY2A-1       VRNGYGFINR NDTKEDVFVH QTAIKKNNPR KFLRSVGDGE TVEFDVVEGE
FRGY2A-2       VRNGYGFINR NDTKEDVFVH QTAIKKNNPR KFLRSVGDGE TVEFDVVEGE
FRGY2B         VRNGYGFINR NDSKEDVFVH QTAIKKNNPR KFLRSVGDGE TVEFDVVEGE

FRGY1          KGAEAANVTG PEGVPVQGSK YAADRNHYRR YPRRRGPPRN YQQNYQNNES
FRGY2A-1       KGAEAANVTG PGGVPVKGSR FAPNR...RR FRRRFYRPRA DTAGESGGE.
FRGY2A-2       KGAEAANVTG PGGVPVKGSR FAPNR...RR FRRRFYRPRA DTAGESGGE.
FRGY2B         KGAEAANVTG PGGVPVKGSR FAPNR...RR FRRQFYRPRA DTAGESGGE.

FRGY1          GEKAEENESA PEGDDSNQQR PYHRRRFPPY YTRRPYGRRP QYSNAPVQGE
FRGY2A-1       GVSPEQMSEG ERGEETSPQQ RPQRRRPPPF FYRRRFRRGP RPNNQQNQGA
FRGY2A-2       GVSPEQMSEG ERGEETSPQQ RPQRRRPPPF FYRRRFRRGP RPNNQQNQGA
FRGY2B         GVSPEQMSEG EKGEETSPQQ RPQRRRPPPF FYRRRFRRGP RPNNQQNQGA

FRGY1          EAEG...... ..ADSQGTDE QGRPARQNMY RGFRPRFRRG PPRQRQPREE
FRGY2A-1       EVTEQSENKD PVAPTSEALA SGDDPQRPPP RRFRQRFRRP FRPRPAPQQT
FRGY2A-2       EVTEQSENKD PVAPTSEALA SGDDPQRPPP RRFRQRFRRP FRPRPAPQQT
FRGY2B         EVTDQSENKD PAAPTSEALA SGDGQQRPPP RRFQQRFRRP FRPRPPPPQT

FRGY1          GNEEDKENQG D.ETQSQPPP QRRYRRNFNY RRRR...... ..........
FRGY2A-1       PEGGDGETKA ESGEDPRPEP QRQRNRPYVQ RRRRQGATQV AATAQGEGKA
FRGY2A-2       PEGGDGETKA ESGEDPRPEP QRQRNRPYVQ RRRRQGATQV AATAQGEGKA
FRGY2B         PEGGDGEAKA EG......EP QRQRNRPYVQ RRRRQ....Q PPTVQGESKA

FRGY1          ..PENPKSQD GKETKAAETS AENTSTPEAE QGGAE..... ......
FRGY2A-1       EPTQHPASEE GTPSDSPTDD GAPVQSSAPD PGIADTPAPE ......
FRGY2A-2       EPTQHPASEE GTPSDSPTDD GAPVQVPALF HLPAALDSMG IFGTLQ
FRGY2B         EPSEHPASEE GTPSDAPTDD GAPVETSEAG VEDTTAPE.. ......
```

N-Terminal Domain
Cold Shock Domain

Figure S2: Alignment between FRGY1, mRNP3 (FRGY2b), mRNP4 (FRGY2a, spliced variants 1
and 2)
Credit: Alain Viel, 2018.



Figure S2: Schematic map of FRGY2A/B constructs in pET303-CT-His.

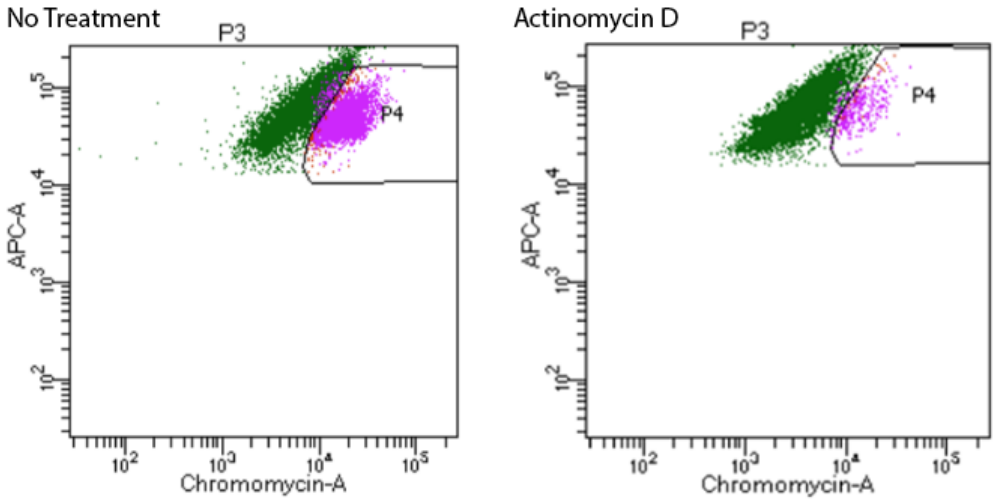


Figure S4. Flow cytometry analysis of nuclei purified from *X. laevis* cells. APC-A: nuclear stain. Chromomycin-A: nucleolar stain. Comparison of untreated nuclei and nuclei treated with actinomycin D (which is known to dissociate nucleoli) shows a marked decrease in nucleoli, while nuclei numbers remain unchanged.

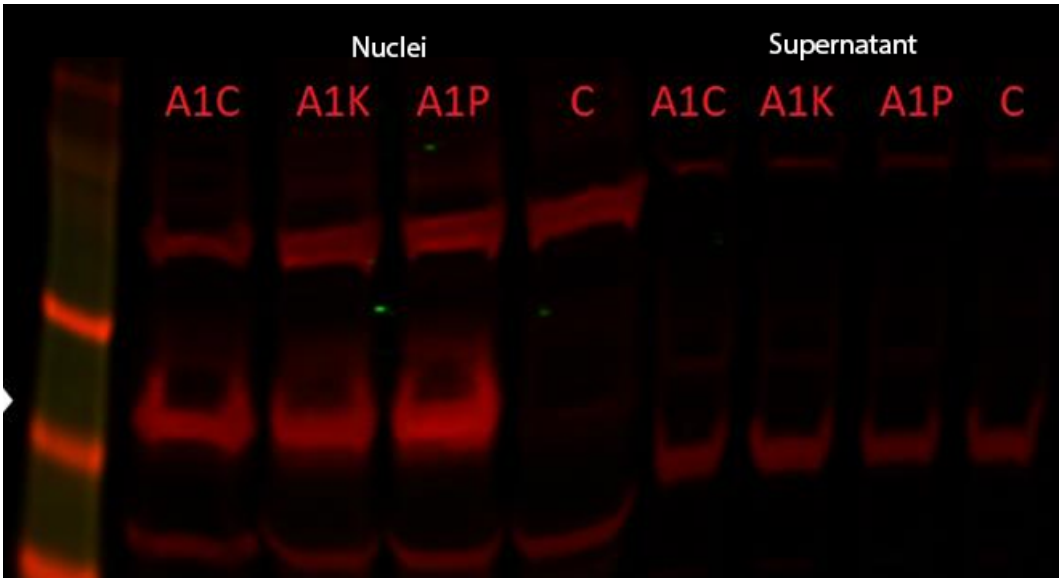


Figure S5. FRGY2A1 nuclear transport. Co-incubation of FRGY2A1 with purified nuclei shows localization of the protein to the nuclei and its absence from the supernatant. A1C: Unmodified FRGY2A1 protein. A1K: Kinase-treated FRGY2A1. A1P: Phosphatase-treated FRGY2A1. C: No protein added.